Journal of the Physical Society of Japan
Vol. 67, No. 4, April, 1998, pp. 1094-1097



# Magnetic Properties of Toroidal Carbon Nanotubes

Ming-Fa LIN

*Department of Physics, National Cheng Kung University, Tainan 70101, Taiwan, The Republic of China*

(Received November 5, 1997)

Persistent currents in thin toroidal carbon nanotubes (TCN's) are linearly periodic functions of magnetic flux ($\phi$) with a period $\phi_0$ ($hc/e$). This result is a manifestation of the Aharonov-Bohm (AB) effect. They depend on the toroid structure (such as curvature, radius, and height), the temperature, and the Zeeman effect. The curvature effect due to the misorientation of $\pi$-electron orbitals affects the electronic states, and thus the persistent current. Consequently, most of armchair-zigzag TCN's exhibit diamagnetism. The current amplitude is inversely proportional to the toroid radius. A temperature increase significantly reduces the persistent current, while the periodical AB oscillation remains unchanged. Measurements of the persistent currents could be used to verify the predicted electronic states and the AB effect.

KEYWORDS: toroidal carbon nanotubes, persistent currents, Aharonov-Bohm effect

Carbon atoms can form diamond, graphite, straight carbon nanotubes (SCN's), toroidal carbon nanotubes (TCN's), $C_{60}$-related fullerenes, and carbon onions. Such systems exhibit rich physical properties. Straight carbon nanotubes, which were discovered by Iijima,[1] represent an interesting class of quasi-one-dimensional systems. Each SCN is a rolled-up graphite sheet in cylindrical form. The radius is $r \sim 10 - 150$ Å, and the length is more than 1 $\mu$m. It is currently possible to produce a uniform nanotube bundle made up of the same single-shell nanotubes.[2] Carbon nanotubes can bend within a crystalline rope. The two ends of the bending nanotubes are able to knit together seamlessly, which leads to the formation of perfect toroidal carbon nanotubes (discovered by Liu *et al.*).[3] The toroid radius ($R \sim 1500 - 2500$ Å) is much larger than the height or the width ($2r \sim 10$ Å). A thin TCN is similar to a mesoscopic metal[4-6] or semiconductor[7] ring. TCN's, as shown for mesoscopic rings, are suitable systems to verify certain quantum effects, *e.g.*, persistent currents. Such currents are caused by magnetic flux ($\phi$) through TCN's. In this work, we mainly study the persistent currents in thin TCN's. Their dependence on magnetic flux, electronic structures, geometric structures (*e.g.*, curvature, radius, and height), and temperature ($T$), and Zeeman splitting is investigated.

A TCN could be regarded as a graphite sheet rolled from the origin simultaneously to the two vectors $\mathbf{R}_x = m\mathbf{a}_1 + n\mathbf{a}_2$ and $\mathbf{R}_y = p\mathbf{a}_1 + q\mathbf{a}_2$ (Fig. 1). $\mathbf{a}_1$ and $\mathbf{a}_2$ are the primitive lattice vectors. The parameters $(m, n, p, q)$ uniquely define a TCN. TCN's which own armchair structures along the transverse direction ($/\!/ \mathbf{R}_x$) as well as zigzag structures along the longitudinal direction ($/\!/ \mathbf{R}_y$), and vice versa, have been studied.[8] They are, respectively, called armchair-zigzag ($(m, m, -p, p)$) and zigzag-armchair ($(m, 0, -p, 2p)$) nanotubes (Fig. 1). For thin TCN's, the electronic states of the latter are insensitive to $\phi$. We will focus on the persistent currents in thin $(m, m, -p, p)$ TCN's. Their width and radius are, respectively, $2r = 3mb/\pi$ and $R = \sqrt{3}\, pb/2\pi$. $b = 1.42$ Å is the C-C bond length.

We consider a TCN which is threaded by a uniform perpendicular $B$ field. Its $\pi$-electron states, as employed for a graphite sheet[9] or a SCN,[10] are calculated by the tight-binding model. The state energies of the $(m, m, -p, p)$ TCN are obtained from diagonalizing the Hamiltonian with only the nearest-neighbor interactions:[8]

$$E(J, L, \phi) = \pm\{\gamma_1^2 \pm 4\gamma_1\gamma_2 \cos(\frac{\pi J}{m}) \cos(\frac{\pi (L + \phi/\phi_0)}{p}) + 4\gamma_2^2 \cos^2(\frac{\pi (L + \phi/\phi_0)}{p})\}^{\frac{1}{2}}. \quad (1)$$

The Zeeman splitting energy $\frac{g\sigma}{m^* R^2} \frac{\phi}{\phi_0}$ can be neglected, except at large $\phi$.[8] A TCN has many discrete states described by the transverse ($J = 1, 2, ..., m$) and the longitudinal ($L = 1, 2, .., p$) angular momenta. ($J_a = m, L_a$) represents the state nearest to the Fermi level. The resonance integrals ($\gamma_1$ and $\gamma_2$ in Fig. 1) along the different directions might differ slightly, which is due to the curvature effect from the misorientation of the $\pi$-electron orbitals.[11-13] $\gamma_1 = (1 - b^2/8r^2)\gamma_0$ and $\gamma_2 = (1 - b^2/32r^2)\gamma_0$,[11] where $\gamma_0 = 3.033$ eV is the resonance integral without the curvature effect.[10] + and − signs appearing outside the square-root sign are, respectively, the antibonding and bonding states (the $\pi^*$ and $\pi$ states). The former are unoccupied at $T = 0$, while the latter are occupied. Moreover, + and − signs inside the square-root sign are the unfolded and folded states, respectively.[10] The magnetic flux changes angular momentum $L$ into $L + \phi/\phi_0$. The electronic states can exhibit a periodical oscillation, with a period $\phi_0$, which is the so-called Aharonov-Bohm (AB) effect.

At $\phi = 0$, there are four types of TCN's according to energy gap. $E_g$ is the energy difference between

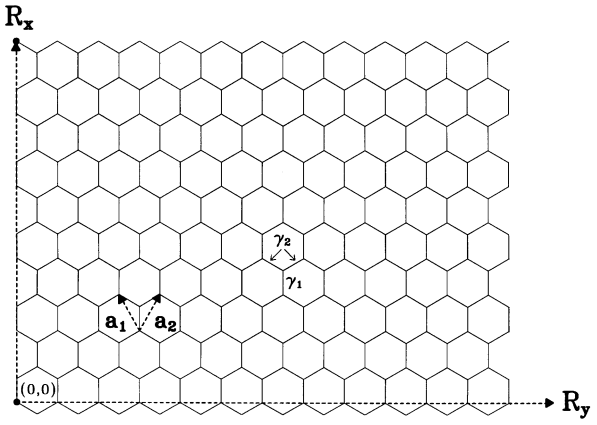


Fig. 1. A toroidal carbon nanotube (TCN) is regarded as a graphite sheet rolled from the origin simultaneously to the vectors $\mathbf{R}_x = m\mathbf{a}_1 + n\mathbf{a}_2$ and $\mathbf{R}_y = p\mathbf{a}_1 + q\mathbf{a}_2$. $\mathbf{a}_1$ and $\mathbf{a}_2$ are the primitive vectors of a graphite sheet.

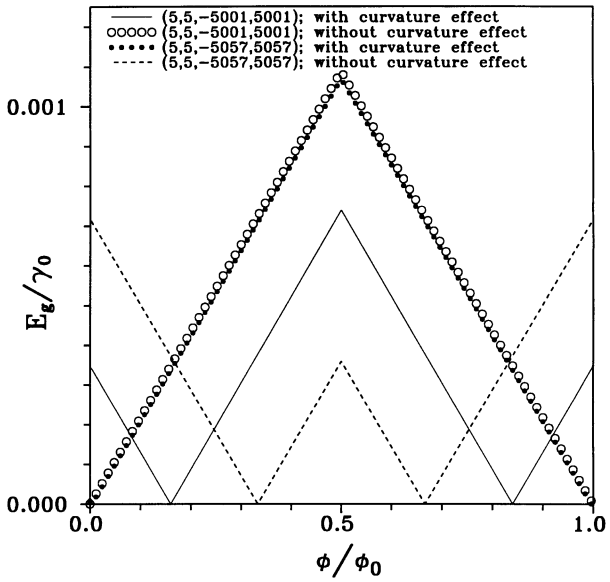


Fig. 2. The $\phi$-dependent energy gap, with or without the curvature effect, is shown for two TCN's: $(5, 5, -5001, 5001)$ and $(5, 5, -5057, 5057)$.

the highest occupied states and the lowest unoccupied state. The type I, II, III, and IV TCN's,[8] which are, respectively, characterized by $E_g \sim \gamma_0\, b/r$, $\sim 0$, $\sim \gamma_0\, b/R$, and $\sim 3\gamma_0\, b^2/16r^2$. For thin TCN's, type II and type III correspond to armchair-zigzag TCN's, while others are zigzag-armchair TCN's. The curvature effect causes many $(m, m, -3i, 3i)$ TCN's to change from type II into type III. Hence, most of armchair-zigzag TCN's belong to type III. For example, the $(5, 5, -5001, 5001)$ TCN, as seen in Fig. 2, has a narrow (vanishing) energy gap in the presence (absence) of the curvature effect. Very few $(m, m, -p, p)$ TCN's have a vanishing energy gap, *e.g.*, the $(5, 5, -5057, 5057)$ TCN (the solid circles in Fig. 2). The curvature effect affects the electronic states and thus the persistent currents.

A $(m, m, -p, p)$ TCN can drastically change from a semiconductor to a metal or vice versa as $\phi$ varies. The $\phi$-dependent energy gap calculated from eq. (1) is given by

$$\begin{aligned} E_g(\phi) &= 2\gamma_0\, |(1 - \frac{b^2}{8r^2}) \\ &\quad \pm 2(1 - \frac{b^2}{32r^2})\, \cos(\frac{\pi\,(L_a + \phi\,/\phi_0\,)}{p})| \\ &= \frac{3b\gamma_2}{R}\, |\frac{\phi}{\phi_0} - \frac{\phi_a}{\phi_0}| \text{ for } 0 \le \phi \le \phi_0\,/2\,. \end{aligned} \tag{2}$$

$\phi_a$ is the magnetic flux corresponding to $E_g = 0$. $E_g(\phi)$, as shown in Fig. 2, is symmetric about $\phi_0\,/2$ and exhibits a linear AB oscillation. Due to the curvature effect, $L_a$ and $\phi_a$ are unequal to $2p/3$ (or $(2p \pm 1)/3$) and $0\ \phi_0$ (or $\phi_0\,/3$), respectively. It is thus difficult to obtain an energy gap from geometric structures. That is to say, the simple rule, $p = 3i$ or $p \neq 3i$, is not available in identifying the electronic states of the thin $(m, m, -p, p)$ TCN's.[8] This result implies that there is no simple relation between geometric structures and persistent currents in the presence of the curvature effect.

The electronic states vary with the magnetic flux, which, therefore, induces a persistent current in a TCN.[4-7] Such current is a variation of the free energy with magnetic flux. The free energy is

$$F(\phi\,, T) = \sum_{J,L} \frac{-2}{\beta}\, \ln\{1 + \exp(-\beta\, E(J, L, \phi\,))\}\,, \tag{3}$$

where $\beta = 1/k_{\mathrm{B}}T$. The factor of 2 accounts for the two spin states. The persistent current is calculated from the definition

$$\begin{aligned} I(\phi\,, T) &= -c\frac{\partial\, F(\phi\,, T)}{\partial\phi} \\ &= -2c \sum_{J_a = m, L} f(E(m, L, \phi\,))\, \frac{\partial\, E(m, L, \phi\,)}{\partial\phi}\,, \end{aligned} \tag{4a}$$

where

$$f(E(m, L, \phi\,)) = \{\exp[\beta\,(E(m, L, \phi\,) - \mu\,(T, \phi\,))] + 1\}^{-1}, \tag{4b}$$

and

$$\frac{\partial\, E(m, L, \phi\,)}{\partial\phi} = \frac{\mp\, 2\pi\gamma_0 \sin(\frac{\pi\,(L + \phi\,/\phi_0\,)}{p})\, [\mp\gamma_1 + 2\gamma_2 \cos(\frac{\pi\,(L + \phi\,/\phi_0\,)}{p})]}{p\phi_0\, |\gamma_1 \mp 2\gamma_2\, \cos(\frac{\pi\,(L + \phi\,/\phi_0\,)}{p}|}\,. \tag{4c}$$

The principal contributions come from the $(J_a = m, L)$ states. The $J \neq m$ states are far from the Fermi level, so the net currents due to them are negligible. The chemical potential $\mu\,(T, \phi\,)$ in the Fermi-Dirac function (eq. (4b)) is equal to zero for any $T$ and $\phi$. That the $\pi$ states are symmetric, about the Fermi level $E_F = 0$, to the $\pi^*$ states is the main reason.

We first see the persistent current at $T = 0$. It is due to the $\pi$ states with $E \le 0$. The current is periodic with a period $\phi_0$ and antisymmetric about $\phi_0\,/2$ (Fig. 3), which

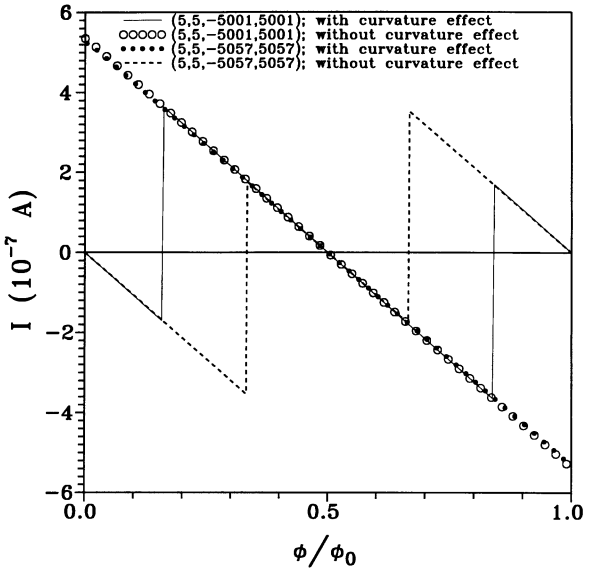


Fig. 3. Persistent currents, with or without the curvature effect, are shown for two TCN's: $(5,5,-5001,5001)$ and $(5,5,-5057,5057)$.

follows from $I(\phi\,) = I(\phi + \phi_0\,) = -I(\phi_0 - \phi\,)$ (eq. (4)). By the detailed calculations (see below), the persistent current is

$$I(\phi\,) = I_0(\delta_{\phi=\phi_a} - 2\phi\,/\phi_0\,) \text{ for } 0 \le \phi \le \phi_0\,/2, \quad (5)$$

where $I_0 = 4\sqrt{3}\pi\gamma_0/p\phi_0$ is the amplitude of the AB oscillation, *e.g.*, $I_0 \sim 5.38 \times 10^{-7}$ A for the $(5,5,-5001,5001)$ TCN. It is noted that $I_0$ can also be expressed as $4ev_F/2\pi R$ ($v_F = 3\gamma_0\, b/2$). $I_0$ is similar to that in mesoscopic metal or semiconductor rings.[4-7] The main difference is that TCN's have a larger Fermi velocity and an additional factor of 2 from the folded and unfolded states. The magnetic response of TCN's are thus stronger than that of mesoscopic rings. The $\phi$-dependence of $I$ will be demonstrated to be linear. Moreover, there is a special jump structure at $\phi_a$, where the metal-semiconductor transition occurs. Equation (5) is suitable for any $(m,m,-p,p)$ TCN, whether or not the curvature effect is taken into account. The only difference is that $\phi_a$ is altered by curvature effect.

The current in eq. (4c) can be evaluated from the small-$\phi$ expansion because of $\pi\phi\,/p\phi_0 \ll 1$. According to the denominator in eq. (4c), the various $L$'s states are divided into $1 \le L + \phi/\phi_0 < L_b + \phi_b/\phi_0$, $L_b + \phi_b/\phi_0 \le L + \phi/\phi_0 < L_a + \phi_a/\phi_0$, and $L + \phi/\phi_0 \ge L_a + \phi_a/\phi_0$. $(L_a, L_b, \phi_a, \phi_b)$ satisfies $E(m, L_a, \phi_a) = E(m, L_b, \phi_b) = 0$, $\phi_b = \phi_0 - \phi_a$, and $L_b = p - 1 - L_a$. $L_a$ and $L_b$ are, respectively, close to $2p/3$ and $p/3$. For the $1 \le L + \phi/\phi_0 < L_b + \phi_b/\phi_0$ states, the current of the unfolded state ($-$ inside the square bracket of eq. (4c)) is the same with that of the folded state ($+$ in eq. (4c)). It is

$$\frac{-I_0}{\sqrt{3}}\{\sin(\frac{\pi\, L}{p}) + \frac{\pi\phi}{p\phi_0}\cos(\frac{\pi\, L}{p})\}. \quad (6)$$

Similar results are obtained for the $L + \phi\,/\phi_0 \ge L_a + \phi_a\,/\phi_0$ states. The current carried by the unfolded or the folded state is

$$\frac{I_0}{\sqrt{3}}\{\sin(\frac{\pi\, L}{p}) + \frac{\pi\phi}{p\phi_0}\cos(\frac{\pi\, L}{p})\}. \quad (7)$$

However, for the $L_b + \phi_b\,/\phi_0 \le L + \phi\,/\phi_0 < L_a + \phi_a\,/\phi_0$ states, the unfolded and the folded states, respectively, carry currents similar to eqs. (6) and (7). The net current from these two states eventually vanishes.

The first terms in eqs. (6) and (7) can cancel each other for the two states $L$ and $p - L$, except for the states $L_a + \phi_a\,/\phi_0$ and $L_b + \phi_b\,/\phi_0$. The significant cancellation is the main cause of the weak magnetic response. The $L_a$ and $L_b$ states, as seen in Fig. 3, induce a special jump of $I_0$ at $\phi_a$ and $\phi_b$, respectively. Concerning the second terms in eqs. (6) and (7), the net current due to them is $-2I_0\phi\,/\phi_0$ after the summation of $L$'s. Hence, the $\phi$-dependent persistent current decreases at a rate of $-2I_0/\phi_0$ and exhibits a jump of $I_0$ at $\phi_a$ or $\phi_b$.

A TCN is paramagnetic (diamagnetic) when the persistent current is positive (negative) at $\phi \to 0$. The type II (III) TCN's with $E_g(\phi = 0) = 0$ ($E_g(\phi = 0) \ne 0$), which exhibit a jump of $I_0$ at $\phi_a = 0$ ($\phi_a \ne 0$), are paramagnetic (diamagnetic). The curvature effect, as stated earlier, changes many $(m,m,-3i,3i)$ TCN's into type III TCN's, and magnetism changes from paramagnetism into diamagnetism, *e.g.*, $I(\phi\,)$ of the $(5,5,-5001,5001)$ TCN in Fig. 3. Most of TCN's exhibit diamagnetism except a small number of TCN's, *e.g.*, the $(5,5,-5057,5057)$ TCN. These results further illustrate that the persistent current directly reflects the features of the electronic states.

In addition to curvature, the persistent current depends on other geometric structures such as height and radius. The toroid height affects $\phi_a$ (eq. (2)), and thus the position of the jump structure, but not the amplitude of the current. $I_0$, as shown in Fig. 4, is inversely proportional to radius, so the induced magnetic moment is proportional to radius. The larger the TCN is, the stronger the magnetic response is. A larger TCN is relatively suitable for experimental verification. The magnetic moment of a TCN is $\sim 5 \times 10^{-20}$ A m$^2$ for a TCN with $R \sim 2000$ Å, which is larger than that ($< 10^{-20}$ A m$^2$) in a mesoscopic metal or semiconductor ring.[4-7] Persistent currents in TCN's can be verified from magnetic measurements.

Also noted that the Zeeman effect is important at large $\phi$, *e.g.*, $\phi \sim 100\ \phi_0$ (or $B \sim 3$ T).[8] It can make certain states touch the Fermi level at magnetic-flux smaller and larger than $\phi_a$, mainly due to the energy difference between spin-up and spin-down states. As a result, there are two jumps of $I_0/2$ at the neighborhood of $\phi_a$, and the period $\phi_0$ of the AB oscillation is destroyed.

When temperature increases from zero, electrons can occupy the $\pi^*$ states with $E \ge 0$. These states produce a current whose direction differs from that of the $\pi$ states. The cancellations among them obviously increase with $T$. Consequently, the jump structures are replaced by the peak structures, and the current amplitude rapidly decreases $T$ increases (Fig. 5). However, the periodical AB oscillation remains similar. The persistent current becomes too small to be observable at higher temperature, *e.g.*, $T \ge 10$ K. The low-temperature magnetic

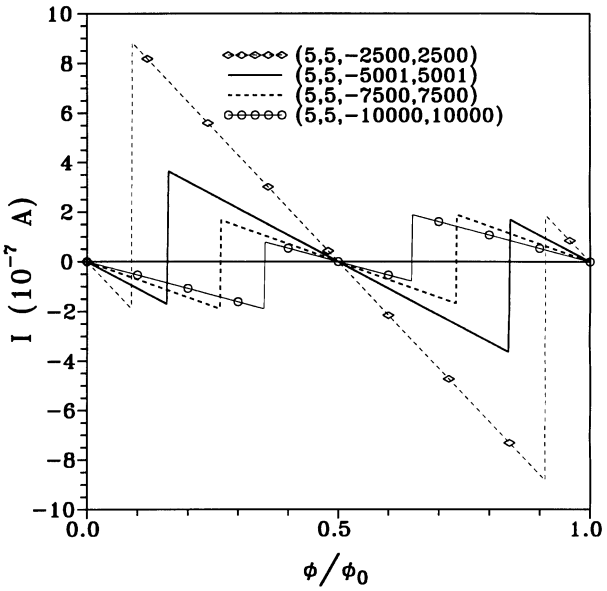


Fig. 4. Persistent currents are shown for various TCN's.

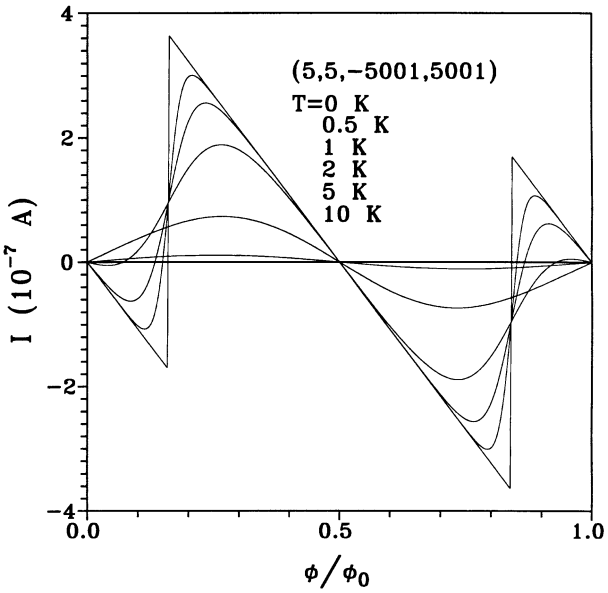


Fig. 5. The persistent current of the $(5, 5, -5001, 5001)$ TCN is shown at different temperatures.

measurement is necessary to verify the persistent current.

A comparison between TCN's and SCN's[14-16] is further made. They exhibit similar magnetisn at $\phi \to 0$. TCN's or SCN's, which are semiconductors (metals) at $\phi = 0$, are paramagnetic (diamagnetic). However, the dependence on nanotube radius, temperature, and Zeeman effect might be different. The magnetic moment in TCN's are proportional to radius, while that in SCN's is independent of radius.[14, 15] The former is observable at $T \leq 10$ K, which is much lower than that ($T < 300$ K)[16] for the latter. The Zeeman splitting induces more jumps for TCN's, but special cusps for SCN's.[16] The difference in special structures is due to the fact that density of states of TCN's and SCN's, respectively, diverge in $\delta$-function and $1/\sqrt{E}$ forms.

In summary, the persistent currents in thin armchair-zigzag TCN's are studied. They are the linearly periodical functions of magnetic flux, with a period $\phi_0$, which is a manifestation of AB effect. They directly reflect the characteristics of electronic states. They depend on the toroid structure (curvature, radius, and height), the temperature, and the Zeeman effect. The curvature effect due to the misorientation of $\pi$-electron orbitals causes most of armchair-zigzag TCN's to exhibit diamagnetism. The current amplitude is inversely proportional to the toroid radius. The toroid height only affects its position. A temperature increase significantly reduces current, while the periodical AB oscillation remains similar. In addition, if the disorder in TCN's is obvious, its effects on currents are similar to those caused by temperature.[4] Such effects need to be further investigated. The Zeeman effect, which might destroy the periodicity of the AB oscillation, is strong only at large $\phi$. The magnetic response of a TCN is stronger than that of a mesoscopic metal or semiconductor ring.[4-7] Persistent currents in TCN's are thus expected to be observable with low-temperature magnetic measurements. Such measurements are useful in verifying the predicted electronic states[8] and the AB effect.

## Acknowledgments

This work was supported in part by the National Science Council of Taiwan, the Republic of China under Grant No. NSC 87-2112-M-006-019.

1) S. Iijima: Nature **354** (1991) 56.
2) A. Thess *et al.*: Science **273** (1996) 438.
3) J. Liu, H. Dai, J. H. Hafner, D. T. Colbert, R. E. Smalley, S. J. Tans and C. Dekker: Nature **385** (1997) 780.
4) H. F. Cheung, Y. Gefen, E. K. Riedel and W. H. Shih: Phys. Rev. B **37** (1988) 6050.
5) L. P. Levy, G. Dolan, J. Dunsmuir and H. Bouchiat: Phys. Rev. Lett. **64** (1990) 2074.
6) V. Chandrasekhar, R. A. Webb, M. J. Brady, M. B. Ketchen, W. J. Gallagher and A. Kleinsasser: Phys. Rev. Lett. **64** (1991) 3578.
7) D. Mailly, C. Chapelier and A. Benoit: Phys. Rev. Lett. **70** (1993) 2020.
8) For the details of the $\pi$-electron states see M. F. Lin and D. S. Chuu: J. Phys. Soc. Jpn. **67** (1998; to be published).
9) P. R. Wallace: Phys. Rev. **71** (1947) 622.
10) R. Saito, M. Fujita, G. Dresselhaus and M. S. Dresselhaus: Appl. Phys. Lett. **60** (1992) 2204; Phys. Rev. B **46** (1992) 1804.
11) C. L. Kane and E. J. Mele: Phys. Rev. Lett. **78** (1997) 1932.
12) J. W. Mintwire, B. I. Dunlap and C. T. White: Phys. Rev. Lett. **68** (1992) 631.
13) N. Hamada, S. I. Sawada and A. Oshiyama: Phys. Rev. Lett. **68** (1992) 1579.
14) H. Ajiki and T. Ando: J. Phys. Soc. Jpn. **62** (1993) 2470; *ibid.* **64** (1995) 4382.
15) J. P. Lu: Phys. Rev. Lett. **74** (1995) 1123.
16) M. F. Lin and K. W.-K. Shung: Phys. Rev. B **52** (1995) 8423.